

# In Vivo Assessment of Bone Healing following Piezotome® Ultrasonic Instrumentation

Jonathan Reside, DDS, MS;\* Eric Everett, MS, PhD;† Ricardo Padilla, DDS, MS;‡ Roger Arce, DDS, PhD;§ Patricia Miguez, DDS, PhD;§ Nadine Brodala, DDS, MS;\* Ingeborg De Kok, DDS, MS;\* Salvador Nares, DDS, PhD††

---

---

## ABSTRACT

**Purpose:** This pilot study evaluated the molecular, histologic, and radiographic healing of bone to instrumentation with piezoelectric or high speed rotary (R) devices over a 3-week healing period.

**Material and Methods:** Fourteen Sprague-Dawley rats (Charles River Laboratories International, Inc., Wilmington, MA, USA) underwent bilateral tibial osteotomies prepared in a randomized split-leg design using Piezotome® (P1) (Satelec Acteon, Merignac, France), Piezotome 2® (P2) (Satelec Acteon), High-speed R instrumentation, or sham surgery (S). At 1 week, an osteogenesis array was used to evaluate differences in gene expression while quantitative analysis assessed percentage bone fill (PBF) and bone mineral density (BMD) in the defect, peripheral, and distant regions at 3 weeks. Qualitative histologic evaluation of healing osteotomies was also performed at 3 weeks.

**Results:** At 1 week, expression of 11 and 18 genes involved in bone healing was significantly ( $p < .05$ ) lower following P1 and P2 instrumentation, respectively, relative to S whereas 16 and 4 genes were lower relative to R. No differences in PBF or BMD were detected between groups within the osteotomy defect. However, significant differences in PBF ( $p = .020$ ) and BMD ( $p = .008$ ) were noted along the peripheral region between P2 and R groups, being R the group with the lowest values. Histologically, smooth osteotomy margins were present following instrumentation using P1 or P2 relative to R.

**Conclusions:** Piezoelectric instrumentation favors preservation of bone adjacent to osteotomies while variations in gene expression suggest differences in healing rates due to surgical modality. Bone instrumented by piezoelectric surgery appears less detrimental to bone healing than high-speed R device.

**KEY WORDS:** gene expression, histology, microCT, Piezoelectric surgery, Piezotome

---

---

---

\*Clinical assistant professor, Department of Periodontology, School of Dentistry, University of North Carolina at Chapel Hill, NC, USA; †professor, Department of Pediatric Dentistry, School of Dentistry, University of North Carolina at Chapel Hill, NC, USA; ‡clinical assistant professor, Department of Diagnostic Sciences, School of Dentistry, University of North Carolina at Chapel Hill, NC, USA; §senior resident, Department of Periodontology, School of Dentistry, University of North Carolina at Chapel Hill, NC, USA; §assistant professor, Department of Periodontics, School of Dental Medicine, University of Pennsylvania, PA, USA; \*\*Department of Prosthodontics, School of Dentistry, University of North Carolina at Chapel Hill, NC, USA; ††associate professor, Department of Periodontology, School of Dentistry, University of North Carolina at Chapel Hill, NC, USA

Reprint requests: Dr. Salvador Nares, Department of Periodontology, School of Dentistry, The University of North Carolina at Chapel Hill, Brauer Hall 111, CB 7450, Chapel Hill, NC 27599-7450, USA; e-mail: salvador\_nares@dentistry.unc.edu

© 2013 Wiley Periodicals, Inc.

DOI 10.1111/cid.12094

## INTRODUCTION

Dental piezoelectric surgical units function by the application of electrical current to polarized quartz or ceramic disks oriented along the long axis of a surgical handpiece. This energy is amplified and transmitted to a surgical tip resulting in linear movement and vibration at frequencies that selectively cut hard tissues. The advantages of piezoelectric surgery in clinical practice have been previously described,<sup>1</sup> and numerous articles have detailed the effectiveness of these units in a variety of dental and medical procedures including lateral window sinus lift techniques,<sup>2-4</sup> autogenous bone grafting,<sup>5-7</sup> dental implant site preparation,<sup>8</sup> tooth extractions,<sup>9,10</sup> periodontal surgery,<sup>11</sup> canal wall mastoidectomy,<sup>12,13</sup> excision of symptomatic ear osteomas,<sup>14</sup> stapedotomy,<sup>15</sup> endoscopic sinus surgery,<sup>16</sup> and head and neck oncological and reconstructive surgery.<sup>17</sup>

Histologically, animal studies have reported a favorable healing response to piezoelectric instrumentation.<sup>18,19</sup> However, it has also been reported that a major clinical limitation is the extra time required to complete the surgery when using these devices.<sup>20</sup> Depending on the bone structure and thickness, osteotomy preparation may require up to fivefold<sup>21</sup> more time compared with conventional instrumentation, thus driving commercial development of more powerful units. While the use of piezoelectric surgical units in dental and medical applications has increased in recent history, little is known regarding the cellular and molecular responses of tissues after ultrasonic instrumentation.

Injury to bony tissues mobilizes a complex sequence of cellular and molecular events that attempt to restore biological form and function. This multistage process incorporates a well orchestrated series of tightly regulated temporal and spatial events involving multiple intracellular and extracellular biological activities<sup>22,23</sup> including mobilization of cellular components and expression of factors linked to inflammation and osteogenesis. The magnitude of this response will be influenced by the extent of injury, and it is likely that exuberant production of proinflammatory molecules following surgical intervention will adversely affect therapeutic outcomes. Specifically, inflammatory cytokines such as interleukin-1, interleukin-6, and tumor necrosis factor- $\alpha$  play critical roles in chemotaxis and angiogenesis as well as in enhancing the synthesis of extracellular matrix.<sup>24,25</sup> However, aberrant inflammatory signaling and associated sequelae have been implicated as important factors in bone injuries that fail to heal.<sup>26</sup> Therefore, employing surgical techniques that minimize trauma during osteotomy preparation may result in more rapid and profound bone healing.<sup>8</sup>

The purpose of this present study is to compare and contrast the healing responses of osteotomies prepared with two generations of piezoelectric surgical units to rotary (R) instrumentation using molecular, radiographic, and histologic approaches in a rat tibia model.

## MATERIALS AND METHODS

### Surgical Procedures

All experimental procedures followed a protocol approved by the Institutional Animal Care and Use Committee. Fourteen male Sprague-Dawley rats

(Charles River Laboratories International, Inc., Wilmington, MA, USA) weighing approximately 250 to 300 g were used for the study for a total of 28 tibiae. Rats were anesthetized with an intraperitoneal injection of ketamine/xylazine and the surgical sites shaved and disinfected with Betadine® (Purdue Products L.P., Stamford, CT, USA). An incision was made along the medial aspect of each tibia and tissues elevated. Using a randomized approach, a 6 mm vertical osteotomy was prepared through the cortical bone in the medial aspect of each tibia using copious saline irrigation and either (1) the BS1 insert (Satelec Acteon, Merignac, France) mounted on the Piezotome® (P1; Satelec Acteon) surgical unit (P1 group,  $n = 8$ ), (2) the BS1 insert mounted on the Piezotome 2® (P2; Implant Center 2 LED, Satelec Acteon) surgical unit (P2 group,  $n = 7$ ), or (3) a  $1/4$  round bur (Brassler, Savannah, GA, USA) with high speed R instrumentation (Implant Center 2 LED) (R group,  $n = 10$ ). The power and irrigation settings were as follows: P1, Mode 1, 50 mL/min irrigation; P2, Mode D1, 60 mL/min irrigation; and R, 200,000 revolutions per minute, 60 mL/min irrigation. Surgical sham control surgeries (S group,  $n = 3$ ) consisted of tissue reflection to expose bone for approximately 3 minutes (the time for incision, soft tissue reflection, and osteotomy preparation). Following surgery, the periosteal/muscle tissues were sutured using 5-0 chromic gut followed by closing of flaps with 4-0 silk suture. Analgesics were administered for 48 hours postoperatively to minimize pain or discomfort and animals monitored daily for any signs of distress over the 3-week period.

Rats were randomly selected for gene expression analyses after 1 week healing ( $n = 6$  rats; 12 tibiae total; 3 tibiae per group) or for micro-computed tomography ( $\mu$ CT) and histological analyses ( $n = 8$  rats; 16 tibiae total; 4 tibiae for P1, 5 tibiae for P2, and 7 tibiae for R) at 3 weeks healing and euthanized by CO<sub>2</sub> inhalation. For tibiae undergoing gene expression studies, residual muscle or soft tissues were carefully removed and the limbs resected at the level of articulation, snap frozen in liquid nitrogen, and stored at  $-80^{\circ}\text{C}$ . For tibiae undergoing  $\mu$ CT and histological analysis, postmortem cardiac perfusion fixation was performed using 10% neutral buffered formalin (NBF) and tibiae were dissected at the level of articulations between femurs and tibiae, placed in ice cold 10% NBF for 48 hours, rinsed in phosphate buffered saline, and stored in 70% v/v ethanol at  $4^{\circ}\text{C}$ .

### Ribonucleic Acid (RNA) Isolation, Real-Time Reverse Transcriptase Polymerase Chain Reaction (PCR)

Tibias were pulverized in liquid nitrogen using a mortar and pestle, total RNA extracted using Trizol® (Invitrogen, Carlsbad, CA, USA) and further purified using the miRNeasy Mini Kit (Qiagen, Germantown, MD, USA) according to manufacturer's instructions. RNA integrity was assessed using a NanoDrop ND-1000 spectrophotometer (NanoDrop Technologies, Wilmington, DE, USA) and the 2100 Bioanalyzer (Agilent Technologies, Santa Clara, CA, USA). For each sample, synthesis of complementary deoxyribonucleic acid was completed from 1 µg of total RNA using the Omniscript Kit (Qiagen) and random decamer primers (Applied Biosystems/Ambion, Austin, TX, USA) according to manufacturer's instructions. Quantitative real time PCR (qRT-PCR) was performed using the Rat Osteogenesis RT<sup>2</sup> Profiler™ PCR Array (SABiosciences, Frederick, MD, USA) on an ABI PRISM® 7500 Real-Time PCR Thermal Cycler (Applied Biosystems, Foster City, CA, USA) according to manufacturer's instructions. Cycling conditions included an initial cycle of 2 minutes at 50°C and 10 minutes at 95°C, followed by a 40 cycles of 15 seconds at 95°C and 1 minute at 60°C. Each array contained 84 wells with assays for different genes related to skeletal development, bone mineral metabolism, cell growth and differentiation, extracellular matrix proteins, transcription factors and regulators, and cell adhesion molecules. RT<sup>2</sup> Profiler™ PCR Array Data Analysis program (SABiosciences) was used to calculate threshold cycle (Ct) values. Data was analyzed using the  $2^{-\Delta\Delta Ct}$  method<sup>27</sup> and results were reported as fold change. Differentially expressed genes were subsequently classified by Gene Ontology terms using the Gene Ontology website <http://www.geneontology.org/>.

### µCT Analysis

Following fixation, tibias were scanned using the Skyscan 1074HR microCT (Skyscan, Aartselaar, Belgium) using the Skyscan acquisition and the NRecon reconstruction software at a resolution of 20.5 µm/pixel. Standardized scanning (40 kV source voltage, 1000 µA source current, 540-millisecond exposure, 206 projections per 180° rotation) and reconstruction settings were used to produce cross-sectional images. All images had a pixel size of 20.7 µm x 20.7 µm with 20.7 µm distance between consecutive cross-sectional images. For calibration and to determine bone mineral densities within regions of interest

(ROIs), hydroxyapatite phantoms (Computerized Imaging Reference Systems, Inc., Norfolk, VA, USA) of 500 mg/cc and 1000 mg/cc densities were utilized under identical scanning and reconstruction parameters. The defect midpoint was identified in the long axis of each tibia, and analyses were completed to include the defect 2 mm proximal to the midpoint and 2 mm distal to the midpoint, for a total defect length of 4 mm (194 of 511 cross-sectional images). Three separate ROIs were selected for analysis representing the central defect and two peripheral regions (Figure 1). Each ROI was selected at 200% within the axial cross-section images approximating the margins of the cortical bone and analysis was completed on any material contained within the ROI. For the ROI corresponding to the central defect, the width of the ROI was measured to correspond to the width of the instrument used to create the cortical osteotomy (0.50 mm for the 1/4 round bur used in R instrumentation and 0.60 mm for the BS1 insert used in P1 and P2 instrumentation). Two peripheral ROIs with a width of 0.25 mm immediately adjacent to the defect ROI were evaluated to assess the effects of the different instrumentation methods on peripheral bone. A distant ROI with a width of 0.25 mm on a surface without periosteal soft tissue elevation or osteotomy preparation

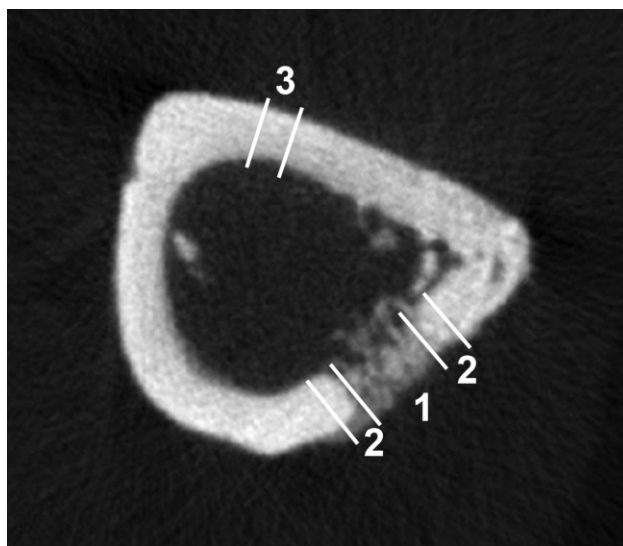


**Figure 1** Regions of interest selections for micro-computed tomography (µCT) analysis. µCT cross-section of the tibiae 3 weeks after ultrasonic osteotomy preparation demonstrating measured region of interest selections for µCT analysis with the CTAn software (Bruker-MicroCT, Kontich, Belgium). The widths of the defect regions of interest (region 1) were 0.50 mm for rotary instrumentation and 0.60 mm for both Piezotome, Piezotome 2 instrumentations. The widths of the bone flanking the osteotomy sites (labeled as 2), and the distant bone site (labeled as 3) were each 0.25 mm.

was also evaluated to compare the effects of different instrumentation methods on distant bone. Bone volume fraction and the average volumetric mineral density of the mineralized tissue (BMD in mg/cc) were quantified. For each sample, the values for the two peripheral regions were averaged prior to statistical analyses.

### Histology

After  $\mu$ CT analysis, tibias were processed for hematoxylin and eosin (H&E) staining. Tissues were demineralized by immersion in Immunocal (Decal Chemical Corporation, Tallman, NY, USA) for 2 weeks at room temperature. Complete decalcification was confirmed by lack of radiopacity. Tissues were routinely processed, paraffin embedded, and the specimens axially sectioned at a thickness of 5  $\mu$ m, deparaffinized, and stained with H&E for gross light microscopic analysis. Samples were qualitatively assessed using an Olympus BX41 optical microscope at 4X and 10  $\times$  magnification (Olympus Optical Company, Ltd, Tokyo, Japan).

### Statistical Analysis

For qRT-PCR data, gene expression group differences were identified using the web-based RT<sup>2</sup> Profiler™ PCR Array Data Analysis program (SABiosciences). Alpha values <0.05 were used for all tests to indicate statistical significance.

Statistical analyses of  $\mu$ CT data was performed using SPSS® 17.0 software (SPSS, Inc., Chicago, IL, USA). The one-way ANOVA statistical test was used to evaluate differences in the percentage of bone fill (PBF) and BMD in the defect and peripheral ROIs. Tukey post hoc analysis was used to identify statistically significant differences ( $p$  values  $\leq$  .05) between the groups. For each region of interest, equivalence testing was completed using 95% confidence intervals compared with a zone of clinical indifference determined by the standard deviation following R instrumentation.

## RESULTS

All rats healed unremarkably with no notable post-operative complications or signs of distress observed between groups throughout the duration of the 3-week healing period. Overall, there was no evidence of any exuberant inflammatory events or notable differences in the inflammatory response between groups. Similarly, there was no evidence of any pathological features, radiographically or histologically.

### 1 Week Real-Time Reverse Transcriptase PCR

Of the 84 genes examined, 28 had significant differences ( $p < .05$ ) in expression when comparing P1 and P2 with S (Table 1) while 19 had significant differences ( $p < .05$ ) in expression when compared with R (Table 2). At 1 week, the expression of genes linked to osseous wound healing was lower in the P1 and P2 groups relative to S and R groups. When compared to S, decreased expression of three genes (*Comp*, *Smad3*, *Vegfa*) and increased expression of one gene (*Col3a1*) was noted in the R group. In comparison, the expression of 18 genes (*Bmpr1a*, *Col4a1*, *Col5a1*, *Col6a1*, *Col12a1*, *Col14a1*, *Fgfr1*, *Fn1*, *Gdf10*, *Igf1*, *Itgav*, *Itgb1*, *Mmp2*, *Scarb1*, *Smad1*, *Tgfb3*, *Tnf*, *Tuft1*) and 11 genes (*Bmp6*, *Bmp7*, *Bmpr1a*, *Col14a1*, *Gdf10*, *Igf1r*, *Itg3*, *Itgam*, *Mmp8*, *Smad1*, *Tuft1*) were significantly decreased in the P1 and P2 groups, respectively, relative to S. No genes were significantly upregulated following P1 or P2 instrumentation relative to S. When R was used as a reference group, the expression of 16 genes (*Anxa5*, *Bgn*, *Bmp4*, *Col3a1*, *Col4a1*, *Col5a1*, *Col6a1*, *Col12a1*, *Col14a1*, *Igf1*, *Itgav*, *Itgb1*, *Msx1*, *Scarb1*, *Smad1*, *Tgfb3*) was significantly lower in the P1 group compared with only 4 genes (*Col14a1*, *Itgam*, *Tgfb1*, *Tgfb3*) with statistically significant lower expression levels following use of the P2 unit. There was a statistically upregulation of one gene (*Egf*) following osteotomy preparation with the P1 unit; no significant upregulation was present following P2 instrumentation.

### 3-Week $\mu$ CT Analysis: PBF (%) and BMD (mg/cc) in Osteotomy Defect, Immediately Adjacent Periphery, and Distant Regions

In the central osteotomy defect regions, there were no statistically significant differences ( $p = .830$ ) in the PBF following instrumentation with P1 ( $31.63 \pm 15.94\%$ ), P2 ( $36.87 \pm 15.64\%$ ), and R ( $32.73 \pm 11.56\%$ ). However, compared with R ( $59.43 \pm 12.89\%$ ), there was a statistically significant increase in PBF in the peripheral region immediately adjacent to the central osteotomy following instrumentation with P2 ( $79.70 \pm 10.32\%$ ;  $p = .020$ ), but not with P1 ( $72.13 \pm 7.50\%$ ;  $p = .198$ ) (Table 3). There was no statistically significant difference in PBF between P1 and P2 treatment groups ( $p = .577$ ). Relative to distant regions, there were statistically significant differences in the PBF in osteotomy defect and immediately peripheral regions for all three treatment groups.

**TABLE 1 Gene Regulation following P1, P2, or R Instrumentation Compared with S at 1 Week Postsurgery**

Gene	Gene Name	Relevant Gene Ontology Term	R Fold Regulation	P1 Fold Regulation	P2 Fold Regulation
<i>Bmp6</i>	Bone morphogenetic protein 6	Osteoblast differentiation	-1.13	-1.34	-1.61*
<i>Bmp7</i>	Bone morphogenetic protein 7	Positive regulation of osteoblast differentiation	-1.52	-1.40	-2.52*
<i>Bmpr1a</i>	Bone morphogenetic protein receptor, type IA	Positive regulation of bone mineralization	-1.20	-1.33*	-1.45*
<i>Col3a1</i>	Collagen, type III, alpha 1	Collagen fibril organization	1.38*	-1.47	-1.011
<i>Col4a1</i>	Collagen, type IV, alpha 1	Epithelial cell differentiation	1.03	-1.70*	-1.41
<i>Col5a1</i>	Collagen, type V, alpha 1	Collagen fibril organization	1.06	-1.43*	-1.14
<i>Col6a1</i>	Collagen, type VI, alpha 1	Protein heterotrimerization	1.07	-1.91**	-1.53
<i>Col12a1</i>	Collagen, type XII, alpha 1	Cell adhesion	-1.03	-1.67**	-1.17
<i>Col14a1</i>	Collagen, type XIV, alpha 1	Cell adhesion	1.31	-2.33*	-1.36**
<i>Comp</i>	Cartilage oligomeric matrix protein	Extracellular matrix organization	-2.04*	1.02	-1.19
<i>Fgfr1</i>	Fibroblast growth factor receptor 1	Chondrocyte development	-1.19	-1.41*	-1.46
<i>Fn1</i>	Fibronectin 1	Cell adhesion	-1.05	-1.65**	-1.40
<i>Gdf10</i>	Growth differentiation factor 10	Regulation of ossification	-1.29	-1.56*	-1.86**
<i>Igf1</i>	Insulin-like growth factor 1	Positive regulation of osteoblast differentiation	1.06	-1.58**	-1.32
<i>Igf1r</i>	Insulin-like growth factor 1 receptor	Positive regulation of cell migration	-1.07	-1.46	-1.70*
<i>Itga3</i>	Integrin, alpha 3	Cell adhesion	-1.24	-1.52	-2.04*
<i>Itgam</i>	Integrin, alpha M	Cell adhesion	-1.08	-1.57	-1.89*
<i>Itgav</i>	Integrin, alpha V	Cell adhesion	1.11	-1.67*	-1.25
<i>Itgb1</i>	Integrin, beta 1	Cell adhesion	1.04	-1.38*	-1.26
<i>Mmp2</i>	Matrix metalloproteinase 2	Tissue remodeling	-1.02	-1.99*	-1.5
<i>Mmp8</i>	Matrix metalloproteinase 8	Proteolysis	-1.33	-1.55	-2.09*
<i>Scarb1</i>	Scavenger receptor class B, member 1	Blood vessel endothelial cell migration	1.09	-1.39*	-1.24
<i>Smad1</i>	SMAD family member 1	BMP signaling pathway	-1.20	-1.82**	-1.82*
<i>Smad3</i>	SMAD family member 3	Osteoblast development	-1.45*	-1.21	-1.44
<i>Tgfb3</i>	Transforming growth factor, beta 3	Positive regulation of bone mineralization	1.04	-1.19*	-1.16
<i>Tnfa</i>	Tumor necrosis factor a	Inflammatory response	1.02	-1.41*	1.08
<i>Tuft1</i>	Tuftelin 1	n/a	-1.22	-1.96*	-2.18**
<i>Vegfa</i>	Vascular endothelial growth factor A	Angiogenesis	-1.39*	1.01	-1.22

\* $p < .05$  compared with S. \*\* $p < .01$  compared with S.

P1, Piezotome; P2, Piezotome 2; R, rotary; S, sham surgery.

In the central osteotomy defect regions, there were no statistically significant differences in BMD between the three treatment groups (P1:  $510 \pm 170$  mg/cc; P2:  $600 \pm 130$  mg/cc; R:  $550 \pm 100$  mg/cc;  $p = .607$ ). However, similar to PBF, there was a statistically significant increase in BMD in the peripheral region immediately adjacent to the osteotomy following instrumentation with P2 ( $980 \pm 80$  mg/cc;  $p = .008$ ) compared with R ( $790 \pm 100$  mg/cc), but not with the P1 ( $900 \pm 80$  mg/cc;  $p = .160$ ) (Table 4). Similarly, there was

no statistically significant difference in BMD between P1 and P2 treatment groups ( $p = .403$ ).

As expected, there were statistically significant differences in BMD of the central osteotomy defect for all three treatment groups relative to distant regions. However, there was a statistically significant decrease in BMD between the immediately adjacent periphery and distant regions following R instrumentation ( $p < .0001$ ). Equivalence testing supported the statistical analyses, indicating that the three treatment groups are equivalent

**TABLE 2 Gene Regulation following P1 or P2 Instrumentation Compared with R at 1 Week Postsurgery**

Gene	Gene Name	Relevant Gene Ontology Term	P1 Fold Regulation	P2 Fold Regulation
<i>Anxa5</i>	Annexin A5	Response to organic substance	-1.53*	-1.35
<i>Bgn</i>	Biglycan	Blood vessel remodeling	-1.35*	-1.25
<i>Bmp4</i>	Bone morphogenetic protein 4	Osteoblast differentiation	-1.52*	-1.62
<i>Col3a1</i>	Collagen, type III, alpha 1	Collagen fibril organization	-1.94**	-1.33
<i>Col4a1</i>	Collagen, type IV, alpha 1	Epithelial cell differentiation	-1.76*	-1.45
<i>Col5a1</i>	Collagen, type V, alpha 1	Collagen fibril organization	-1.52**	-1.21
<i>Col6a1</i>	Collagen, type VI, alpha 1	Protein heterotrimerization	-2.03**	-1.63
<i>Col12a1</i>	Collagen, type XII, alpha 1	Cell adhesion	-1.62**	-1.13
<i>Col14a1</i>	Collagen, type XIV, alpha 1	Cell adhesion	-3.07*	-1.80*
<i>Egf</i>	Epidermal growth factor	Ossification	2.47**	1.23
<i>Igf1</i>	Insulin-like growth factor 1	Positive regulation of osteoblast differentiation	-1.68*	-1.40
<i>Itgam</i>	Integrin, alpha M	Cell adhesion	-1.46	-1.75*
<i>Itgav</i>	Integrin, alpha V	Cell adhesion	-1.86**	-1.39
<i>Itgb1</i>	Integrin, beta 1	Cell adhesion	-1.44**	-1.31
<i>Msx1</i>	Msh homeobox 1	BMP signaling pathway	-1.51*	-1.61
<i>Scarb1</i>	Scavenger receptor class B, member 1	Blood vessel endothelial cell migration	-1.51*	-1.35
<i>Smad1</i>	SMAD family member 1	BMP signaling pathway	-1.52*	-1.52
<i>Tgfb1</i>	Transforming growth factor, beta 1	Growth factor activity	-1.52	-1.69*
<i>Tgfb3</i>	Transforming growth factor, beta receptor III	BMP signaling pathway	-1.54*	-1.53*

\**p* < .05 compared to R. \*\**p* < .01 compared to R. P1, Piezotome; P2, Piezotome 2; R, rotary.

in regard to PBF and BMD in the central osteotomy and distant sites. Nonequivalence, however, is suggested between R and P2 in regard to BMD in sites immediately peripheral to the osteotomy.

**Descriptive Histology of Bone Healing at 3 Weeks**

Histologically, the healing of the osteotomies was very similar among the P1 and P2 groups at 3 weeks.

Bone healing correlated with the radiographic findings (Figures 1A–C and 2). Furthermore, there were minimal differences apparent in the newly formed bone within the osteotomy defects following the three different treatment modalities. However, in a number of sections in which R instrumentation was performed (Figure 2C), the remodeling process appeared to extend laterally relative to the osteotomy site, a feature not characteristic of the osteotomy sites prepared

**TABLE 3 Percentage of Bone Fill (PBF) and Bone Mineral Density (BMD, mg/cc) at 3 Weeks within Three Regions of Interest as Determined by μCT Analysis**

Treatment	Region of Interest					
	Defect		Periphery		Distant	
	Bone Fill (%)	Bone Mineral Density (mg/cc)	Bone Fill (%)	Bone Mineral Density (mg/cc)	Bone Fill (%)	Bone Mineral Density (mg/cc)
P1 ( <i>n</i> = 4)	31.63 ± 15.94	0.51 ± 0.17	72.13 ± 7.50	0.90 ± 0.08	97.51 ± 2.32	1.02 ± 0.10
P2 ( <i>n</i> = 5)	36.87 ± 15.64	0.60 ± 0.13	79.70 ± 10.32*	0.98 ± 0.08**	98.18 ± 0/90	1.07 ± 0.08
R ( <i>n</i> = 7)	32.73 ± 11.56	0.55 ± 0.10	59.43 ± 12.89	0.79 ± 0.10	98.68 ± 1.50	1.07 ± 0.07

\**p* < .05 within location compared to R. \*\**p* < .01 within location compared to R. P1, Piezotome; P2, Piezotome 2; R, rotary.

**TABLE 4 Percentage of Bone Fill (PBF) and Bone Mineral Density (BMD, mg/cc) at 3 Weeks within Treatment Groups as Determined by  $\mu$ CT Analysis**

ROI	Treatment					
	P1 (n = 4)		P2 (n = 5)		R (n = 7)	
	Bone Fill (%)	Bone Mineral Density (mg/cc)	Bone Fill (%)	Bone Mineral Density (mg/cc)	Bone Fill (%)	Bone Mineral Density (mg/cc)
Defect	31.63 $\pm$ 15.94**	0.51 $\pm$ 0.17**	36.87 $\pm$ 15.64**	0.60 $\pm$ 0.13**	32.73 $\pm$ 11.56**	0.55 $\pm$ 0.10**
Periphery	72.13 $\pm$ 7.50*	0.90 $\pm$ 0.08	79.70 $\pm$ 10.32*	0.98 $\pm$ 0.08	59.43 $\pm$ 12.89**	0.79 $\pm$ 0.10**
Distant	97.51 $\pm$ 2.32	1.02 $\pm$ 0.10	98.18 $\pm$ 0.90	1.07 $\pm$ 0.08	98.68 $\pm$ 1.50	1.07 $\pm$ 0.07

\* $p < .05$  within treatment group compared with distant location. \*\* $p < .01$  within treatment group compared to distant location. P1, Piezotome; P2, Piezotome 2; R, rotary.

by piezoelectric instrumentation. Following P1 (Figure 2A) or P2 (Figure 2B) instrumentation, the osteotomy margins were smooth and much better defined in a majority of the samples at 3 weeks, suggesting minimal postoperative necrosis of the marginal bone during the healing process following piezoelec-

tric instrumentation. This feature was inconsistently identified in the samples following R instrumentation (Figure 2C). In all samples, osteoblasts lined the inner aspect of the bone, including the newly formed bone within the defect. Incremental lines were present indicating bone apposition at 3 weeks.

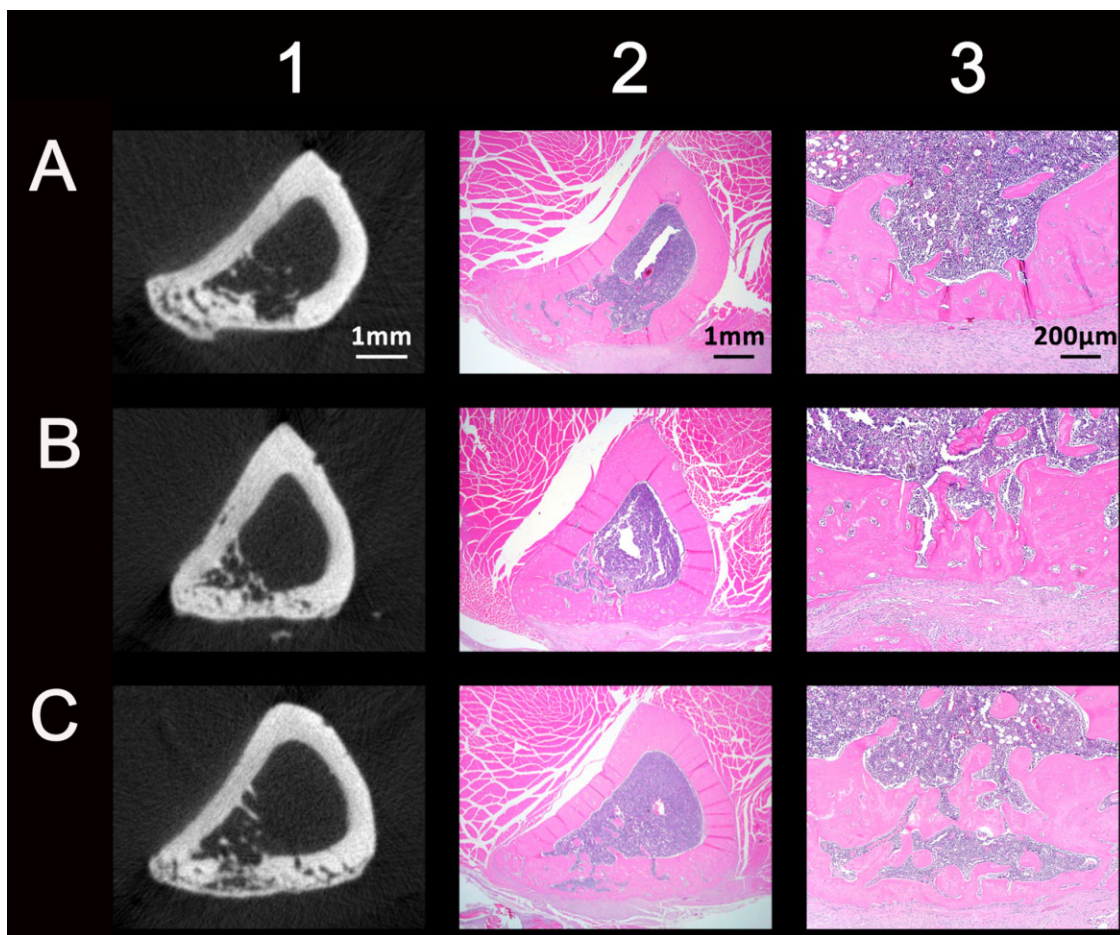


**Figure 2** Comparison of micro-computed tomography and hematoxylin and eosin staining images at 3 weeks postsurgery. Representative views comparing microCT slices (1) and histology sections (2 and 3) at the same level are shown for Piezotome (A), Piezotome 2 (B), and rotary (C).

## DISCUSSION

While the clinical effectiveness of piezoelectric surgery continues to be well documented, the tissue response to this form of surgical instrumentation is not completely understood. We evaluated the early (1 and 3 weeks) osseous healing responses to osteotomies prepared by piezoelectric and conventional R instrumentation using molecular, radiographic, and histological approaches. In rat fracture models, it has been reported that the healing process is completed in rats within 5 to 6 weeks<sup>28–30</sup> so that the appropriate time points to analyze the early and late phases of healing are between 1 and 2 weeks and 4 to 6 weeks, respectively.<sup>31</sup> And while we did not specifically use the fracture model, these points serve as a basis for investigating the healing of osseous injuries in rats.

Over the course of the study, there were no detectable differences in animal behavior after instrumentation with any of the treatment modalities. As expected, we noted that osteotomies performed with P2 were faster than with P1 raising the possibility that the added power output may be detrimental to osseous tissues and/or may impede the healing process. However, we did not identify any genetic, histologic, or radiographic evidence of necrosis or exuberant inflammation over the course of the 3-week healing period. Histologically, the margins of the osteotomy surfaces were exceptionally smooth following instrumentation with either P1 or P2.

We evaluated the early genetic response of osseous tissues using a focused osteogenesis PCR array. In mouse fracture models, the expression of proinflammatory cytokines and matrix proteins peaks within 24 hours declining to very low levels in approximately 3 days after injury. Sequential peaks in the expression of genes important in the chondrogenic and osteogenic phases of remodeling occur at day 7 and at days 14 to 21, respectively.<sup>32</sup> However, to the best of our knowledge, no literature has been published detailing the stages of osseous healing and temporal gene expression patterns following experimental tibial osteotomies using piezoelectric instrumentation. In general, we noted that after a 1-week healing period, gene expression linked to bone remodeling at sites prepared by P1 and P2 remained active in 1 week, but at a lesser degree compared with S controls or R instrumentation. This does not necessarily indicate that bone healing is impaired following instrumentation with P1 and P2

relative to S or R. Rather, it is possible that expression of genes important in bone regeneration and remodeling may have occurred earlier following piezoelectric instrumentation. In contrast, expression of these genes continues for longer periods following R instrumentation. Given the kinetic differences between gene expression and protein production, and more significantly between gene expression and tissue maturation and mineralization,<sup>33</sup> it is likely that the divergence of the cellular and molecular events observed in this study was triggered by the chosen method of bone manipulation. In agreement,  $\mu$ CT analysis of week 3 osteotomies identified statistically significant increases in PBF and BMD along the peripheral aspect of the osteotomies prepared by P2 compared with R but not between P1 and P2. This suggests that viability of cells and tissue formation immediately adjacent to osteotomies is more favorable when prepared using piezoelectric instrumentation. Alternatively, the piezo tip itself and/or the energy imparted upon it during osteotomy preparation is more biologically favorable relative to R instrumentation. To exclude the possibility of a dull bur contributing to osseous trauma, each osteotomy preparation using R instrumentation was performed using a fresh bur. Taken together, this implies that the choice of surgical modality impacts the rate of osseous healing with piezoelectric instrumentation yielding lower levels of bone trauma compared with traditional R instrumentation.

The biological manifestations of our observations are not completely understood but are likely the result of residual bone microstructure and local tissue responses. Previous studies have described factors that may influence osseous healing including temperature, postinstrumentation damage to bone microstructure, and blood perfusion.<sup>34</sup> Bone necrosis occurs during osteotomy preparation when the bone temperature exceeds 47°C for 1 minute.<sup>35</sup> Harder and colleagues reported that P1 produced a median temperature increase of 1.2°C, while other ultrasonic piezoelectric units examined produced median temperature increases of 2.5 to 3.1°C on bone specimens at room temperature (21°C).<sup>36</sup> In these laboratory conditions, the bone temperature increases during piezoelectric instrumentation are below that necessary to cause necrosis. In addition, while a benefit of piezoelectric surgery improved visibility stemming from the cavitation effect, there is no evidence that intraosseous vascular thrombosis or occlusion of

adjacent bone occurs following piezoelectric instrumentation.<sup>34</sup> Consequently, blood supply to the remaining osseous tissue appears to be preserved. Although we did not evaluate these specific factors, the apparent lack of tissue necrosis histologically suggests that they were minimally impacted.

Evidence suggests that microcracks form during plastic deformation of bone and act to mechanically damage canalicular spaces and promote osteocyte apoptosis.<sup>37,38</sup> Damage to canalicular spaces during osteotomy preparation may be expected to have a similar effect on osteocyte viability. Following piezoelectric ultrasonic instrumentation, bone microstructure and the vitality of osteocytes adjacent to the cut surface are preserved.<sup>39</sup> In normal bone homeostasis, osteocyte cell death promotes osteoclast recruitment and subsequent resorption through complex cell signaling during the initial stages of repair.<sup>40</sup> Maintenance of peripheral cellular vitality may act to minimize cellular signaling processes contributing to osseous resorptive processes, while the intact bony margins may provide a solid surface for osteoblasts adherence and osteoid deposition. Indeed, bone apposition was readily apparent on peripheral surfaces forming an osseous bridge spanning the outer aspect of the osteotomy defect. While the defect margins were identifiable histologically on numerous specimens, the newly regenerated bone was largely in direct contact with the previously excised bone and in some locations indistinguishable from preexisting bone.

Our genetic findings, when examined in conjunction with the  $\mu$ CT and histological data, suggest that the expression of osteogenic factors following R instrumentation requires a prolonged and more robust response relative to piezoelectric instrumentation. As such, differences in the rates of healing will influence the gene expression patterns among the different treatment groups at any particular time. It is also possible that the differences in healing between R and piezoelectric surgical modalities may be influenced by their effects on peripheral osseous structures adjacent to the osteotomy, potentially influencing not only the rate of healing within the osteotomy site, but also the timing, duration, and degree of gene expression. Surgical modalities causing injury to peripheral osseous tissues or inducing peripheral bone resorption may necessitate increased gene expression levels to overcome the insult. Assuming that piezoelectric instrumentation results in fewer

changes to adjacent bone, the downregulation in *Bmp4* and *Tgfb $\beta$ 3* at 1 week may, in part, be explained by this theory.

This study has limitations. We used 14 rats which yielded 28 tibias for analysis over a 3-week time period. Larger studies with more collection points are required as is quantitative analysis of immunohistochemical staining. Further study evaluating the effects of piezoelectric instrumentation at a cellular level, specifically on osteocyte and osteoblast function, would help to underline potential differences in surgical modalities. Nevertheless, our study indicates that bone instrumented by piezoelectric surgery shows less detrimental effects to bone than high speed R device and that the higher power output of the P2 is a safe upgrade from P1. Indeed, this study also demonstrates greater bone fill and mineralization at the wound margins in sites instrumented by P2 suggesting faster healing relative to R. Additional kinetic studies are required to confirm this finding.

## ACKNOWLEDGMENTS

The authors would like to thank Ms. Sandra Horton for her technical assistance with the study. This study was funded by an unrestricted research grant from Acteon, Inc., Merignac, France.

## CONFLICT OF INTEREST

All authors declare no conflict of interest.

## REFERENCES

1. Labanca M, Azzola F, Vinci R, Rodella LF. Piezoelectric surgery: twenty years of use. *Br J Oral Maxillofac Surg* 2008; 46:265–269.
2. Sohn DS, Lee JS, An KM, Choi BJ. Piezoelectric internal sinus elevation (PISE) technique: a new method for internal sinus elevation. *Implant Dent* 2009; 18:458–463.
3. Vercellotti T, De Paoli S, Nevins M. The piezoelectric bony window osteotomy and sinus membrane elevation: introduction of a new technique for simplification of the sinus augmentation procedure. *Int J Periodontics Restorative Dent* 2001; 21:561–567.
4. Wallace SS, Mazor Z, Froum SJ, Cho SC, Tarnow DP. Schneiderian membrane perforation rate during sinus elevation using piezosurgery: clinical results of 100 consecutive cases. *Int J Periodontics Restorative Dent* 2007; 27:413–419.
5. Happe A. Use of a piezoelectric surgical device to harvest bone grafts from the mandibular ramus: report of 40 cases. *Int J Periodontics Restorative Dent* 2007; 27:241–249.

6. Sohn DS, Ahn MR, Lee WH, Yeo DS, Lim SY. Piezoelectric osteotomy for intraoral harvesting of bone blocks. *Int J Periodontics Restorative Dent* 2007; 27:127–131.
7. Stubinger S, Robertson A, Zimmerer KS, Leiggenger C, Sader R, Kunz C. Piezoelectric harvesting of an autogenous bone graft from the zygomaticomaxillary region: case report. *Int J Periodontics Restorative Dent* 2006; 26:453–457.
8. Preti G, Martinasso G, Peirone B, et al. Cytokines and growth factors involved in the osseointegration of oral titanium implants positioned using piezoelectric bone surgery versus a drill technique: a pilot study in minipigs. *J Periodontol* 2007; 78:716–722.
9. Degerliyurt K, Akar V, Denizci S, Yucel E. Bone lid technique with piezosurgery to preserve inferior alveolar nerve. *Oral Surg Oral Med Oral Pathol Oral Radiol Endod* 2009; 108:e1–e5.
10. Grenga V, Bovi M. Piezoelectric surgery for exposure of palatally impacted canines. *J Clin Orthod* 2004; 38:446–448.
11. Vercellotti T, Pollack AS. A new bone surgery device: sinus grafting and periodontal surgery. *Compend Contin Educ Dent* 2006; 27:319–325.
12. Crippa B, Salzano FA, Mora R, Dellepiane M, Salami A, Guastini L. Comparison of postoperative pain: piezoelectric device versus microdrill. *Eur Arch Otorhinolaryngol* 2011; 268:1279–1282.
13. Salami A, Mora R, Dellepiane M, Guastini L. Piezosurgery for removal of symptomatic ear osteoma. *Eur Arch Otorhinolaryngol* 2010a; 267:1527–1530.
14. Salami A, Mora R, Dellepiane M, Crippa B, Santomauro V, Guastini L. Piezosurgery versus microdrill in intact canal wall mastoidectomy. *Eur Arch Otorhinolaryngol* 2010b; 267:1705–1711.
15. Crippa B, Dellepiane M, Mora R, Salami A. Stapedotomy with and without piezosurgery: 4 years' experience. *J Otolaryngol* 2010; 39:108–114.
16. Bolger WE. Piezoelectric surgical device in endoscopic sinus surgery: an initial clinical experience. *Ann Otol Rhinol Laryngol* 2009; 118:621–624.
17. Crosetti E, Battiston B, Succo G. Piezosurgery in head and neck oncological and reconstructive surgery: personal experience on 127 cases. *Acta Otorhinolaryngol Ital* 2009; 29:1–9.
18. Perfetti G, Calderini M, Berardi D, Leoni S, Ferrante M, Spoto G. Evaluation of non-specific tissue alkaline phosphatase on bone samples from traditional and piezoelectric osteotomy. *J Biol Regul Homeost Agents* 2006; 20:67–72.
19. Vercellotti T, Nevins ML, Kim DM, et al. Osseous response following resective therapy with piezosurgery. *Int J Periodontics Restorative Dent* 2005; 25:543–549.
20. Schaller BJ, Gruber R, Merten HA, et al. Piezoelectric bone surgery: a revolutionary technique for minimally invasive surgery in cranial base and spinal surgery? Technical note. *Neurosurgery* 2005; 57 (Suppl):E410.
21. Kotrikova B, Wirtz R, Krempien R, et al. Piezosurgery—a new safe technique in cranial osteoplasty? *Int J Oral Maxillofac Surg* 2006; 35:461–465.
22. Einhorn TA. The cell and molecular biology of fracture healing. *Clin Orthop Relat Res* 1998; 355 (Suppl):S7–S21.
23. Sandberg MM, Aro HT, Vuorio EI. Gene expression during bone repair. *Clin Orthop Relat Res* 1993; 289:292–312.
24. Ai-Aql ZS, Alagl AS, Graves DT, Gerstenfeld LC, Einhorn TA. Molecular mechanisms controlling bone formation during fracture healing and distraction osteogenesis. *J Dent Res* 2008; 87:107–118.
25. Gerstenfeld LC, Cho TJ, Kon T, et al. Impaired fracture healing in the absence of TNF-alpha signaling: the role of TNF-alpha in endochondral cartilage resorption. *J Bone Miner Res* 2003; 18:1584–1592.
26. Mountziaris PM, Spicer PP, Kasper FK, Mikos AG. Harnessing and modulating inflammation in strategies for bone regeneration. *Tissue Eng Part B Rev* 2011; 17:393–402.
27. Livak KJ, Schmittgen TD. Analysis of relative gene expression data using real-time quantitative PCR and the  $2^{-(\Delta\Delta C_T)}$  method. *Methods* 2001; 25:402–408.
28. Schmidmaier G, Wildemann B, Melis B, et al. Development and characterization of a standard closed tibial fracture model in the rat. *Eur J Trauma* 2004; 30:35–42.
29. Claes L, Blakytyn R, Gockelmann M, Schoen M, Ignatius A, Willie B. Early dynamization by reduced fixation stiffness does not improve fracture healing in a rat femoral osteotomy model. *J Orthop Res* 2009; 27:22–27.
30. Einhorn TA. The science of fracture healing. *J Orthop Trauma* 2005; 19:4–6.
31. Histing T, Garcia P, Holstein JH, et al. Small animal bone healing models: standards, tips, and pitfalls results of a consensus meeting. *Bone* 2011; 49:591–599.
32. Cho TJ, Gerstenfeld LC, Einhorn TA. Differential temporal expression of members of the transforming growth factor beta superfamily during murine fracture healing. *J Bone Miner Res* 2002; 17:513–520.
33. Donos N, Hamlet S, Lang NP, et al. Gene expression profile of osseointegration of a hydrophilic compared with a hydrophobic microrough implant surface. *Clin Oral Implants Res* 2011; 22:365–372.
34. von See C, Gellrich NC, Rucker M, Kokemuller H, Kober H, Stover E. Investigation of perfusion in osseous vessels in close vicinity to piezo-electric bone cutting. *Br J Oral Maxillofac Surg* 2012; 50:251–255.
35. Albrektsson T, Eriksson A. Thermally induced bone necrosis in rabbits: relation to implant failure in humans. *Clin Orthop Relat Res* 1985; 195:311–312.
36. Harder S, Wolfart S, Mehl C, Kern M. Performance of ultrasonic devices for bone surgery and associated intraosseous temperature development. *Int J Oral Maxillofac Implants* 2009; 24:484–490.

37. Noble BS, Reeve J. Osteocyte function, osteocyte death and bone fracture resistance. *Mol Cell Endocrinol* 2000; 159:7–13.
38. Rochefort GY, Pallu S, Benhamou CL. Osteocyte: the unrecognized side of bone tissue. *Osteoporos Int* 2010; 21: 1457–1469.
39. Hollstein S, Hoffmann E, Vogel J, Heyroth F, Prochnow N, Maurer P. Micromorphometrical analyses of five different ultrasonic osteotomy devices at the rabbit skull. *Clin Oral Implants Res* 2012; 23:713–718.
40. Nakahama K. Cellular communications in bone homeostasis and repair. *Cell Mol Life Sci* 2010; 67:4001–4009.

Copyright of Clinical Implant Dentistry & Related Research is the property of Wiley-Blackwell and its content may not be copied or emailed to multiple sites or posted to a listserv without the copyright holder's express written permission. However, users may print, download, or email articles for individual use.